Experimental Validation of a Rule-Based Voltage Regulation Algorithm for MV Grids

Georgios C. Kryonidis
Dept. of Electr. & Comput. Eng.
Aristotle University of Thessaloniki
Thessaloniki, Greece
kryonidi@ece.auth.gr

Manuel Barragán-Villarejo
Dept. of Electr. Eng.
Universidad de Sevilla
Sevilla, Spain
manuelbarragan@us.es

Francisco de Paula García-López
Dept. of Electr. Eng.
Universidad de Sevilla
Sevilla, Spain
fdpgarcia@us.es

Kyriaki-Nefeli D. Malamaki
Dept. of Electr. & Comput. Eng.
Aristotle University of Thessaloniki
Thessaloniki, Greece
kyriaki_nefeli@hotmail.com

Juan Manuel Mauricio
Dept. of Electr. Eng.
Universidad de Sevilla
Sevilla, Spain
jmmauricio@us.es

José María Maza-Ortega
Dept. of Electr. Eng.
Universidad de Sevilla
Sevilla, Spain
jmmaza@us.es

Charis S. Demoulias
Dept. of Electr. & Comput. Eng.
Aristotle University of Thessaloniki
Thessaloniki, Greece
chdimoul@auth.gr

***Abstract*—Scope of this paper is to experimentally validate a rule-based control scheme for the voltage regulation of radial medium-voltage (MV) distribution grids with high penetration of distributed renewable energy sources (DRESs). The examined control scheme uses the available reactive power of DRESs to tackle possible voltage violations, while ensuring near-minimum active power losses. This is attained by adopting a time delay allocation method to prioritize the reactive power response of DRESs. This control algorithm is applied to a scaled-down version of the CIGRE European benchmark MV grid to experimentally assess its performance in terms of voltage regulation and optimal network operation.**

***Index Terms*—Distributed renewable energy sources, experimental validation, loss minimization, reactive power control, voltage control.**

I. Introduction

Voltage regulation (VR) is considered as one of the most important technical challenges that distribution system operators (DSOs) should effectively address to achieve high penetration of distributed renewable energy sources (DRESs) [1]. To this end, several solutions have been proposed in the literature dealing with the incorporation of reactive power control (RPC) techniques into DRESs [2]. Furthermore, to improve the overall network performance, the minimization of network losses has been included as an additional operating objective, transforming the conventional VR problem into an optimization problem [3].

Focusing on medium-voltage (MV) distribution grids, the state-of-the-art RPC methods can be classified into model- and data-driven approaches. In the former case, a detailed network model is used as an input in the mathematical formulation of the optimization problem [4]–[6]. Nevertheless, these solutions are characterized by limited applicability under real-field conditions due to the lack of detailed network knowledge from the DSOs [7]. On the contrary, data-driven control strategies are network-agnostic since the reactive power of each DRES is determined by using local and/or remote information without requiring a complete knowledge of the network [8]. Additionally, they are characterized by low computational complexity, facilitating their implementation in real distribution grids.

Regarding data-driven methods, the authors in [9] propose a decentralized RPC technique where the reactive power of each DRES is dynamically adjusted based on local measurements, while also ensuring minimal inter-node interference. Moreover, a model-free solution is adopted in [10] that coordinates the on-load tap changer of the high-voltage/medium-voltage (HV/MV) transformer with the DRESs on multiple time-scales to optimally control the network voltages. In [11], a measurement-based network identification technique is proposed which serves as a basis for the determination of the optimal operating set-points of DRESs. An online distributed control algorithm is presented in [12], where each DRES locally updates the output power by using a closed-form formula to regulate the network voltages while ensuring minimum network losses. Finally, in [13], a rule-based VR method is proposed that uses a time delay allocation procedure based on the graph theory to optimally distribute the reactive power among the DRESs.

As a common drawback, the performance of the vast ma-

This research is funded by the European Union under the Horizon 2020 project EASY-RES (GA 764090). In addition, it was developed under Grant PID2021-124571OB-I00 funded by MCIN/AEI/ 10.13039/501100011033 and by "ERDF A way of making Europe".

Citation information, DOI: 10.1109/POWERTECH55446.2023.10202691

jority of the solutions proposed in the literature has been only assessed via simulations, hiding potential issues that may occur during their application in real or close-to-real environments. Only few works deal with the experimental validation of VR algorithms. Specifically, the authors in [14] evaluate the performance of the coordinated VR scheme proposed in [15]. Nevertheless, their analysis focus only on assessing the central controller by conducting a controller hardware-in-the-loop experiment where the whole system under study is modeled in the digital real-time simulator (DRTS) without using any real equipment. This issue is partially addressed in [16] via power hardware-in-the-loop experiments, where the proposed VR algorithm is integrated into a real DRES converter and evaluated in a system under study modeled in the DRTS. However, possible interactions due to the existence of multiple DRES cannot be evaluated since only one real DRES converter is considered.

To this end, the scope of this paper is to experimentally validate the VR control scheme proposed in [13]. Contrary to [15], [16], the system under study consists of only real equipment, i.e., network lines, DRES converters, etc., thus emulating with high accuracy the behavior of a real distribution grid. In particular, experiments are conducted on a scaled-down version of the CIGRE European benchmark MV grid containing several DRESs and loads to assess the performance of the examined control scheme in terms of VR and optimal network operation.

The remainder of this paper is organized as follows. The examined VR method is presented in Section II, while in Section III the experimental setup is analytically described. Section IV presents the experimental results and, finally, Section V concludes the paper.

II. Examined VR Method

According to the mathematical analysis presented in [13], it was shown that considering the VR of a specific node, the network losses are minimized if the RPC is only undertaken by the DRES connected to this node. To properly apply this outcome in the overvoltage mitigation process of a radial MV network, a new control strategy is introduced which can be summarized in the following statement: Overvoltages can be effectively mitigated with minimum losses if each DRES starts absorbing reactive power only when the voltage at its point of common coupling (PCC) is greater than or equal to the PCC voltage of the next downstream DRES. To implement this concept, a hybrid centralized-decentralized control architecture is introduced; the reactive power set-point of each DRES is determined using only local measurements and a central controller is used to prioritize the response of each DRES. In the next sub-sections, the decentralized control logic that is implemented in each DRES is initially described followed by a detailed presentation of the central controller.

A. RPC of DRESs

Assuming a DRES connected to the i-th node, the output reactive power is determined following the procedure described in Fig. 1. This procedure consists of two operation modes separated by a small dead-band (db) to prevent repeated activation-deactivation cycles. The first operation mode is activated when the PCC voltage of the DRES connected to the i-th node ($V_{\mathrm{pcc},i}$) exceeds the maximum permissible limit ($V_{\max}$). Nevertheless, a time delay ($d_{\mathrm{up},i}$) is applied to the response of the DRES aiming to implement the above-mentioned control concept and achieve a near-optimal reactive power allocation among the DRESs. This is attained by setting different time delays to prioritize the response of the DRESs. It is worth mentioning that these time delays are determined by the central controller using as input the PCC voltage and the location of each DRES. Following this time delay, the DRES starts absorbing reactive power. The amount of the output reactive power is determined by a proportional-integral (PI) controller which is introduced to eliminate the error between the PCC voltage ($V_{\mathrm{pcc},i}$) and the target voltage ($V_{\max}-0.5db$). This process continues till the reactive power capability limit of the DRES is reached ($Q_{\min,i}$) unless either the voltage is successfully controlled or the overall power factor (pf_i) seen from the i-th node and downstream reaches a minimum value ($pf_{\min,i}$) [13]. In the latter two cases, the PI controller aims to maintain a constant power factor.

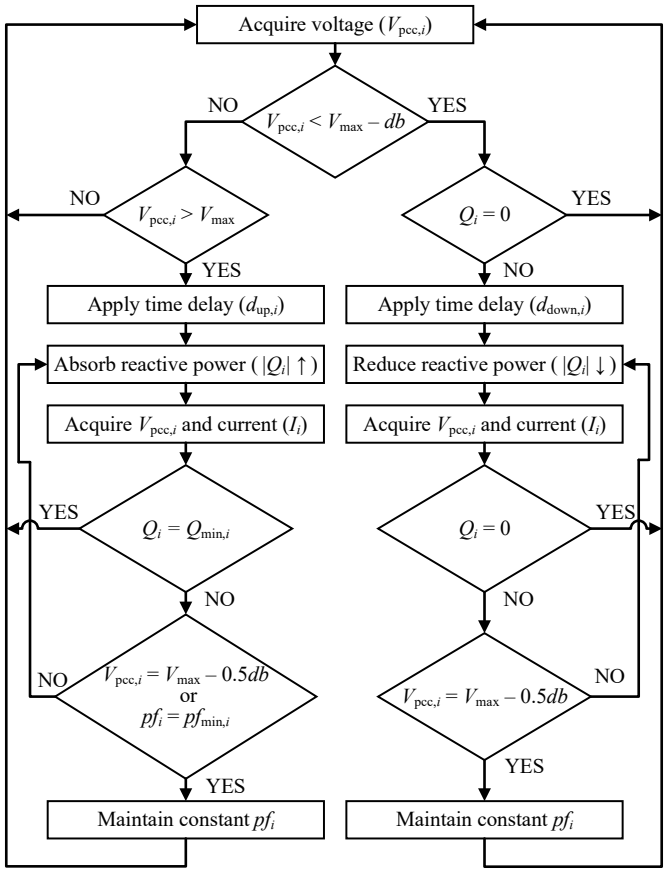

Fig. 1: RPC of the DRES connected to the i-th node.

The second operation mode deals with the reverse process of reducing the reactive power absorption and is activated when

$V_{\mathrm{pcc},i}$ is reduced below the voltage threshold ($V_{\max} - db$). Similarly to the first operation mode, a time delay ($d_{\mathrm{down},i}$) is applied to the activation of this process to ensure a near-optimal reactive power allocation among the DRESs. Following this time delay, the reactive power of the DRES connected to the i-th node is reduced till zero unless the voltage is successfully regulated. In the latter case, the constant power factor operation is activated.

B. Operation of the Central Controller

The scope of the central controller is to coordinate the response of the DRESs participating in the VR process in order to ensure a near-optimal network operation in terms of minimizing active power losses. Towards this objective, the central controller receives at discrete time intervals ($\Delta\tau$) the voltage magnitudes of the DRESs. Note that these time intervals depend on the characteristics of the communication infrastructure and are DSO-defined varying from seconds to minutes, without, however, significantly affecting the performance of the VR. Afterward, the central controller determines the set of time delays (d_{up}, d_{down}) in each DRES to coordinate the activation of the two operation modes among the DRESs. The time delays are updated in every time interval $\Delta\tau$ using the graph theory according to the analysis presented below.

Assuming a given time instant, the received PCC voltages of DRESs are structured in a tree presenting the same topology with the electrical grid. This tree is simplified by removing nodes to form an increasing voltage profile in each path between the root and a leaf node. The DRESs connected to the omitted nodes are not participating in the VR process for the given time instant, since according to the analysis presented in [13], their participation would lead to increased network losses. To set the time delays of the remaining DRESs, the following conditions shall be met:

- The same time delay is applied to the DRESs of the same level nodes to ensure simultaneous RPC activation and equal reactive power sharing among these DRESs.
- In each path between the root and a leaf node, the time delays of the DRESs are sorted based on their PCC voltages. Regarding the first operation mode, high priority, i.e. small time delay, is provided to the DRES with the highest voltage. On the contrary, in the second operation mode, high priority is provided to the DRES with the lowest voltage.

III. Testbed Description

The examined testbed is a simplification of an actual German network proposed by the CIGRE Task Force C06.04.02 to conduct studies related to the DRES integration in MV grids [17]. This network consists of two radial feeders, i.e. feeder 1 and feeder 2, with lengths of of 15 km and 8 km, respectively. In the conducted experiments, feeder 1 was used since it presents a higher voltage sensitivity to power variations compared to feeder 2. The topology of feeder 1 is presented in Fig. 2, where it can be seen that it consists of 11 nodes and 10 branches. A scaled-down version of this network has been built

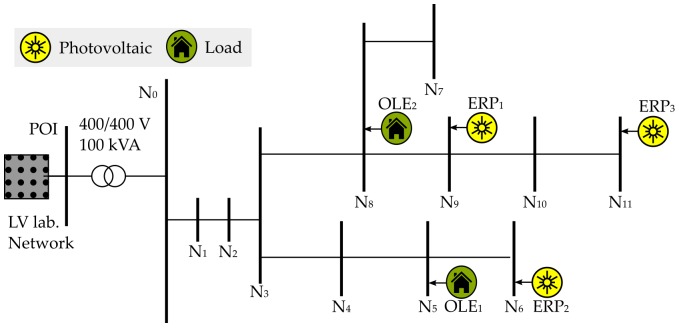

Fig. 2: Topology of the feeder under study (feeder 1) of the CIGRE European benchmark MV grid.

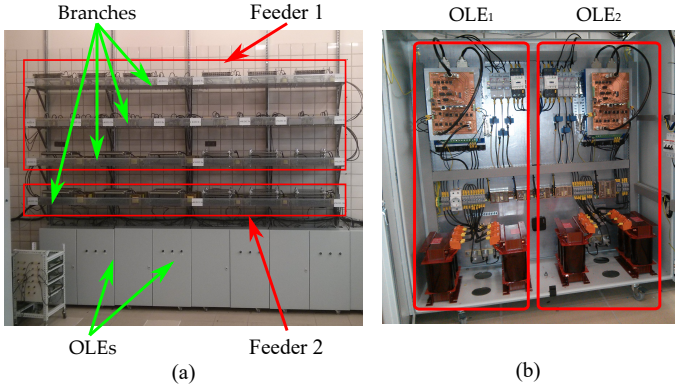

Fig. 3: Implementation of the CIGRE European benchmark MV grid in the USE lab; a) Network overview and b) detail of the OLE electrical cabinet.

TABLE I: Values of the resistors and reactors of each branch within the scaled-down network.

Node 1	Node 2	Resistance (mΩ)	Reactance (mΩ)
N1	N2	60.00	39.25
N2	N3	25.00	15.75
N3	N4	5.00	3.25
N4	N5	10.00	3.25
N5	N6	25.00	7.75
N3	N8	10.00	6.25
N8	N7	25.00	7.75
N8	N9	5.00	1.50
N9	N10	10.00	3.25
N10	N11	5.00	1.50

in the laboratory of the University of Seville. Specifically, the base magnitudes of the original grid were changed from 20 kV and 10 MVA to 400 V and 100 kVA, respectively. This allowed the accurate reproduction of the network performance in the LV lab environment in terms of voltage drops, power flows and power losses in the per unit system. More details regarding the derivation and design of the scaled-down network can be found in [18].

TABLE II: Network Voltages (V).

Node	Experiment	Simulation	Error (%)
N1	222.79	222.79	0.00
N5	223.62	227.20	1.59
N6	226.45	228.58	0.94
N8	224.78	227.84	1.36
N9	225.86	228.38	1.11
N11	227.89	229.21	0.57

The scaled-down version of the CIGRE EUropean MV network is presented in Fig. 3 where the network branches and the Omnimode Load Emulators (OLEs) can be noticed. The parameters of the branches that consist of resistors and reactors are presented in Table I. These values have been calculated to achieve the same voltage drops in the per unit system as in the original network. The interior of a cabinet located at the bottom of Fig. 3a is shown in Fig. 3b. This cabinet contains 2 OLEs, where each one consists of a controllable Voltage Source Coverter (VSC), grid-coupling filter without transformer, measurement units and control devices. OLEs are used to emulate any type of consumption or generation profile, thus providing additional flexibility to perform any type of test. In the conducted experiments, two OLEs are connected to nodes N5 and N8 emulating a commercial and a residential load, respectively. Additionally, three converter prototypes emulating PVs are connected in nodes N6, N9, and N11. These prototypes have been developed in the frame of EASY-RES Horizon 2020 project and can provide a series of ancillary services to the grid [19]. Among them, the VR control strategy of [13] has been incorporated into the EASY-RES prototypes (ERPs) which has been experimentally validated with the results presented in the next section. It is worth mentioning that the technical characteristics of the ERPs are analytically presented in [20].

IV. Experimental Results

As a first step, a comparison is made between simulations and experimental results to identify any potential gap between modeling and real implementation of a VR method. To this end, a static scenario is assumed in the scaled-down network of Fig. 2, where each ERP injects 9 kW to the grid with a leading power factor of 0.9. Additionally, each OLE absorbs 9 kW from the grid with a lagging power factor equal to 0.9. The corresponding results are shown in Table II. It can be observed that there is a good alignment between simulations and experiments, since the corresponding error on the network voltages is less than 2 %. This discrepancy mainly exists due to the uncertainty related to the network parameters and measurement errors. Overall, it can be concluded that the modelling of the network is accurate enough and can adequately represent the actual network performance.

Secondly, a dynamic scenario is assessed where the output power of both PVs (ERPs) and loads (OLEs) follows the 24-hour profile illustrated in Fig. 4. Note that for loads, positive sign indicates absorption from the grid. On the contrary, regarding PVs, positive sign indicates injection to the grid. According to Fig. 4, it can be seen that generation is much higher than demand during midday. This scenario was deliberately created to evaluate the performance of the examined VR method under high DRES penetration. In addition, these profiles have been time-scaled from 24 hours to 15 minutes to reduce testing time. However, the experimental results are shown considering the original 24-hour horizon.

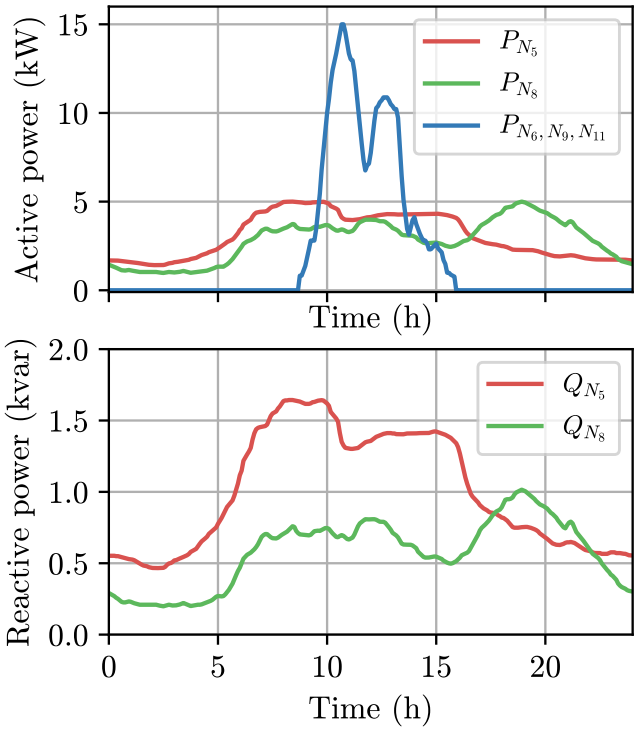

Fig. 4: 24-hour power profiles. (Top): Active power output of PVs (ERPs) and loads (OLEs). (Bottom): Reactive power of loads.

The voltage profiles of the network nodes where the PVs and the loads are connected to are presented in Fig. 5. Two scenarios are considered, namely without and with the examined VR strategy. In the former case, PVs operate at unity power factor and the corresponding voltage profiles are displayed in the top of Fig. 5. Note that the voltage of node N1 is kept constant and equal to 1.05 p.u. by a controllable AC source throughout the test. During non-midday hours, the network voltages remain below the N1 voltage due to small or no power injections by the PVs However, during midday, it is observed that the network voltages are increased exceeding the maximum permissible value ($V_{\max}$) of 1.1 p.u. Specifically, the maximum network voltage is observed at node N6 which slightly exceeds 1.15 p.u. This is due to the fact that the overall PV injection is much higher than the power demanded by the loads leading to high reverse power flows and high network voltages.

In the second scenario, the examined VR strategy is acti-

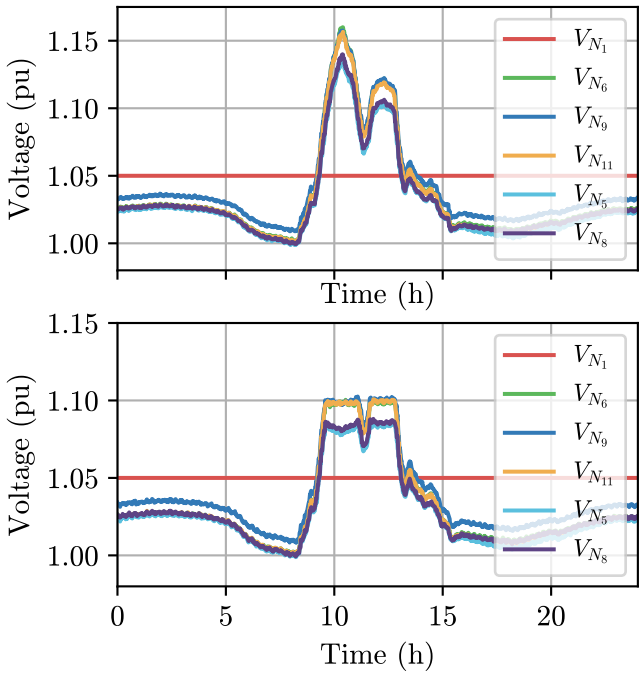

Fig. 5: 24-hour nodal voltages. (Top): Without VR strategy. (Bottom): With the examined VR strategy.

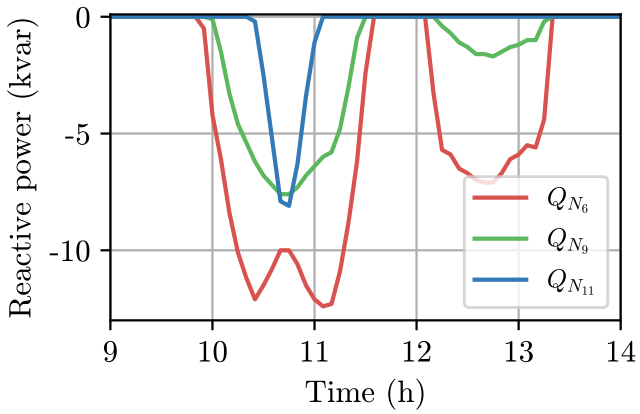

Fig. 6: Output reactive power of PVs (ERPs) during midday.

vated and the PVs participate in the overvoltage mitigation process by absorbing reactive power according to the control concept presented in Section II. The corresponding voltage profiles are presented in the bottom of Fig. 5. During non-midday hours, where the network voltages are below $V_{\max}$, the voltage profiles are identical to the previous scenario. This can be justified by the fact that the examined VR strategy is an event-triggered method, i.e., the reactive power absorption is activated only when the voltages exceed $V_{\max}$, thus leading to reduced reactive power usage and network losses. Contrary to the previous scenario, the voltages of nodes N6, N9, and N11 are kept below or equal to 1.1 p.u., while the rest nodes have lower values despite the high PV injections. This is attributed to the reactive power absorbed by the PVs according to examined VR strategy.

The allocation of reactive power among the PVs during the midday is displayed in Fig. 6. At around 10 a.m., the PV at node N6 starts absorbing reactive power. This PV was selected by the central controller since it presents the maximum network voltage. Thus, according to the analysis presented in Section II, this control action minimizes the amount of reactive power needed to regulate the network voltages and thus ensures the minimization of network losses. A few moments later, the reactive power process is also undertaken by the PV connected to node N9. This is the node with the second highest voltage and its activation is necessary to maintain the nodal voltages at $V_{\max}$ since the single action of the PV at node N6 would not be sufficient to avoid overvoltages. Then, around 10:30 a.m., the PV at node N11 also starts to absorb reactive power. This time coincides with the generation peak as shown in Fig. 4. Therefore, additional reactive power absorption is needed to prevent the nodal voltages from exceeding the limit value $V_{\max}$. From this time onwards, PV generation decreases progressively leading to a reduction of the absorbed reactive power. This reduction continues till it reaches zero at around 11:30 a.m. It should be noted that reactove power reduction as well as the deactivation of this VR process in each PV occurs in the opposite way to its activation, i.e., from PV at node N11 to the PV at node N6. The PV generated increases again at 12:00 p.m. Thus, the corresponding PVs re-activate the reactive power absorption process in the same way as occurred at 10:00 a.m. to maintain the nodal voltages at 1.1 p.u. However, the reactive power absorption is lower, according to the injected PV power. Furthermore, the PV at node N11 does not absorb reactive power, since the reactive power absorbed by the PV at nodes N6 and N9 is enough to maintain the nodal voltages below to or equal to $V_{\max}$. As a result, the amount of the reactive power needed to regulate the network voltages is minimized, leading also to minimum network losses.

Finally, the active and reactive power profiles at node N1 when the VR is deactivated (top plot) and activated (bottom plot) is shown in Fig. 7. Note that these power profiles represent the power exchanged with the upstream/utility grid. When the examined VR strategy is deactivated, the controllable ac source at node N1 has to provide the reactive power demanded by the loads at nodes N5 and N8. Additionally, it can be observed that the direction of the active power changes during the day. In particular, during the midday, generation exceeds demands and the surplus is absorbed by the controllable ac source. The opposite occurs during non-midday hours where generation is smaller than demand and the controllable ac source provides the missing active power to the grid. When the examined VR strategy is activated, the power profiles are affected only during the midday due to the activation of reactive power absorption by the PVs that participate in the VR process. It can be seen that active power is reduced due to the increased network losses caused by the reactive power absorption from the PVs. Nevertheless, as

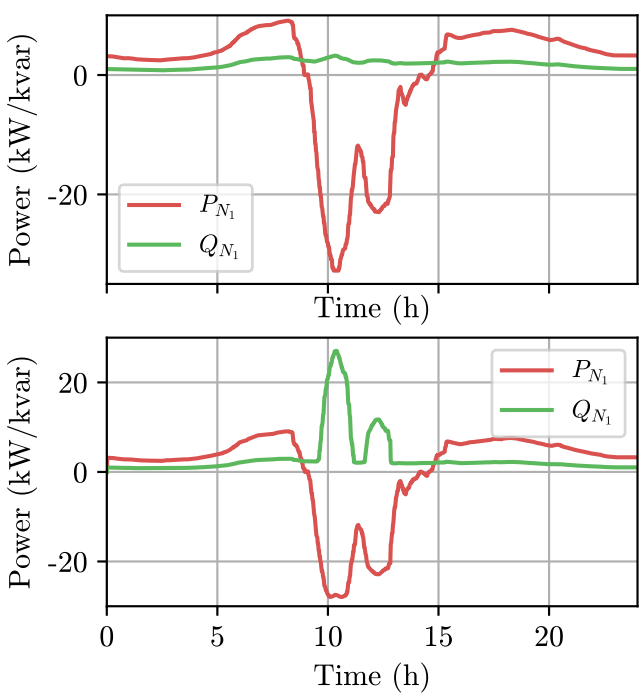

Fig. 7: 24-hour power profiles at node N1. (Top): Without VR strategy. (Bottom): With the examined VR strategy.

shown previously, the examined VR strategy leads to minimum network losses, and thus, the active power presented in the bottom plot of Fig. 7 is the maximum that can be delivered to the upstream grid while maintaining the network voltages within the permissible limits.

V. Conclusions

In this paper, the VR strategy presented in [13] was experimentally validated. Contrary to the current state-of-the-art solutions, experiments took place in a scaled-down version of the CIGRE European MV benchmark grid consisting of only real elements. Static and dynamic scenarios were examined to investigate the performance of the proposed VR strategy. In the former, results revealed a good accuracy between simulations and experiments, while in the latter, the validity of the examined VR strategy was assessed in terms of regulating the network voltages while maintaining minimum network losses. Additionally, no interactions between the ERPs were observed, indicating the feasibility of the examined VR strategy to be applied in real distribution grids.

References

[1] C. L. Masters, "Voltage rise: the big issue when connecting embedded generation to long 11 kv overhead lines," *Power Eng. J.*, vol. 16, no. 1, pp. 5–12, Feb. 2002.

[2] G. C. Kryonidis, E. O. Kontis, T. A. Papadopoulos, K. D. Pippi, A. I. Nousdilis, G. A. Barzegkar-Ntovom, A. D. Boubaris, and N. P. Papanikolaou, "Ancillary services in active distribution networks: A review of technological trends from operational and online analysis perspective," *Renew. Sustain. Energy Rev.*, vol. 147, p. 111198, 2021.

[3] K. E. Antoniadou-Plytaria, I. N. Kouveliotis-Lysikatos, P. S. Georgilakis, and N. D. Hatziargyriou, "Distributed and decentralized voltage control of smart distribution networks: Models, methods, and future research," *IEEE Trans. Smart Grid*, vol. 8, no. 6, pp. 2999–3008, 2017.

[4] T. Hong, D. Zhao, Y. Zhang, B. Cui, and Y. Tian, "Optimal voltage reference for droop-based DERs in distribution systems," *IEEE Trans. Smart Grid*, vol. 11, no. 3, pp. 2357–2366, 2020.

[5] X. Sun, J. Qiu, Y. Tao, Y. Ma, and J. Zhao, "Coordinated real-time voltage control in active distribution networks: An incentive-based fairness approach," *IEEE Trans. Smart Grid*, vol. 13, no. 4, pp. 2650–2663, 2022.

[6] Y. Guo, Q. Wu, H. Gao, S. Huang, B. Zhou, and C. Li, "Double-time-scale coordinated voltage control in active distribution networks based on MPC," *IEEE Trans. Sustain. Energy*, vol. 11, no. 1, pp. 294–303, 2020.

[7] V. Bassi, L. F. Ochoa, T. Alpcan, and C. Leckie, "Electrical model-free voltage calculations using neural networks and smart meter data," *IEEE Trans. Smart Grid*, vol. article in press, pp. 1–1, 2022.

[8] T. T. Mai, A. N. M. Haque, P. P. Vergara, P. H. Nguyen, and G. Pemen, "Adaptive coordination of sequential droop control for PV inverters to mitigate voltage rise in PV-rich LV distribution networks," *Electr. Power Syst. Res.*, vol. 192, p. 106931, 2021.

[9] S. S. M. Reshikeshan, S. L. Matthiesen, M. S. Illindala, A. A. Renjit, and R. Roychowdhury, "Autonomous voltage regulation by distributed pv inverters with minimal inter-node interference," *IEEE Trans. Ind. Appl.*, vol. 57, no. 3, pp. 2058–2066, 2021.

[10] Y. Huo, P. Li, H. Ji, H. Yu, J. Yan, J. Wu, and C. Wang, "Data-driven coordinated voltage control method of distribution networks with high DG penetration," *IEEE Trans. Power Syst.*, article in press.

[11] H. Xu, A. D. Domínguez-García, V. V. Veeravalli, and P. W. Sauer, "Data-driven voltage regulation in radial power distribution systems," *IEEE Trans. Power Syst.*, vol. 35, no. 3, pp. 2133–2143, 2020.

[12] J. Li, Z. Xu, J. Zhao, and C. Zhang, "Distributed online voltage control in active distribution networks considering PV curtailment," *IEEE Trans. Ind. Informat.*, vol. 15, no. 10, pp. 5519–5530, 2019.

[13] G. C. Kryonidis, C. S. Demoulias, and G. K. Papagiannis, "A new voltage control scheme for active medium-voltage (MV) networks," *Electr. Power Syst. Res.*, vol. 169, pp. 53–64, 2019.

[14] A. Newaz, J. Ospina, and M. O. Faruque, "Controller hardware-in-the-loop validation of coordinated voltage control scheme for distribution systems containing inverter-based distributed generation," *IEEE J. Emerg. Sel. Topics Ind. Electron.*, vol. 3, no. 2, pp. 332–341, 2022.

[15] ——, "Coordinated voltage control in distribution systems with distributed generations," in *IEEE Power Energy Soc. Gen. Meeting (PESGM)*, 2019, pp. 1–5.

[16] Y. Wang, M. H. Syed, E. Guillo-Sansano, Y. Xu, and G. M. Burt, "Inverter-based voltage control of distribution networks: A three-level coordinated method and power hardware-in-the-loop validation," *IEEE Trans. Sustain. Energy*, vol. 11, no. 4, pp. 2380–2391, 2020.

[17] K. Rudion, A. Orths, Z. A. Styczynski, and K. Strunz, "Design of benchmark of medium voltage distribution network for investigation of DG integration," in *2006 IEEE Power Engineering Society General Meeting*, 2006, p. 6.

[18] J. M. Maza-Ortega, M. Barragán-Villarejo, F. de Paula García-López, J. Jiménez, J. M. Mauricio, L. Alvarado-Barrios, and A. Gómez-Expósito, "A multi-platform lab for teaching and research in active distribution networks," *IEEE Trans. Power Syst.*, vol. 32, no. 6, pp. 4861–4870, 2017.

[19] K.-N. D. Malamaki, F. Casado-Machado, M. Barragán-Villarejo, A. M. Gross, G. C. Kryonidis, J. L. Martinez-Ramos, and C. S. Demoulias, "Ramp-rate limitation control of distributed renewable energy sources via supercapacitors," *IEEE Trans. Ind. Appl.*, vol. 58, no. 6, pp. 7581–7594, 2022.

[20] J. M. M. Ortega, Y. Khazem, A. Scott, and A. Jindal, "D6.1: Report detailing the implementation of converter prototypes," 2020, EASY-RES H2020 Project.